Supporting Information

Highly efficient and durable aqueous electrocatalytic reduction of CO_2 to HCOOH with a novel Bismuth-MOF: experimental and DFT study

Xurui Zhang[1], Yanxing Zhang[2,3], Qingqing Li[1], Xiaodong Zhou[3], Qingyu Li[4], Jin Yi[1], Yuyu Liu[1,*], Jiujun Zhang[1]

[1] Institute of Sustainable Energy/College of Sciences, Shanghai University, Shanghai 200444, China.

[2] School of Physics, Henan Normal University, Xinxiang, Henan 453007, China

[3] Department of Chemical Engineering, University of Louisiana at Lafayette, Lafayette, Louisiana 70504, United States.

[4] Guangxi Key Laboratory of Low Carbon Energy Materials, School of Chemical and Pharmaceutical Science, Guangxi Normal University, Guilin, Guangxi 541004, China.

*Corresponding author: E-mail: liuyuyu@shu.edu.cn.

Table S1. MOF-based materials for CO_2 electrocatalytic reduction.

Metal–organic framework -based materials	Electrolyte	Electric potential	FE (main products)	Refs
HKUST-1 MOF (= $[Cu_3(BTC)_2 \cdot 3H_2O]_n$)	0.5M $KHCO_3$	−0.9 $V_{Ag/Ag+}$	5.6% (CH_3OH), 10.3% (C_2H_5OH), 15.9% (Total)	1
HKUST-1 MOF	1M KOH	−1.07 V_{RHE}	45% (C_2H_4)	2
HKUST-1 MOF	0.5M $KHCO_3$	−2.0 V_{SCE}	20% (CH_4)	3
	0.5M $KHCO_3$	−1.8 V_{SCE}	16% (C_2H_4)	
HKUST-1 MOF	0.01M TBATFB in DMF	−2.5 $V_{Ag/Ag+}$	51% ($H_2C_2O_4$)	4
Copper porphyrin MOF nanosheets Cu_2(CuTCPP) MOF nanosheets TCPP = 5,10,15,20-tetrakis(4-carboxyphenyl) porphyrin Copper(II)-5,10,15,20-tetrakis(4-carboxyphenyl) porphyrin–Cu(II)	1M H_2O and 0.5M $EMIMBF_4$ in CH_3CN	−1.55 $V_{Ag/Ag+}$ 1.65 $V_{Ag/Ag+}$	68.4% (HCOOH) 85.2% (Total)	5
CuBi12 (= MOF prepared from blends of 79% HKUST-1 and 21% CAU-17)	0.5M $KHCO_3$	−0.21 V_{RHE}	8.6% (CH_3OH), 28.3% (CH_3CH_2OH)	6
Copper rubeanate MOF	0.5M $KHCO_3$	−1.2 V_{SHE}	98% (HCOOH)	7

Oxide-derived Cu/carbon, OD Cu/C-1000	0.1M $KHCO_3$	−0.3 V_{RHE}	43.2% (CH_3OH)	[8]
Cu^{II}/adeninato/carboxylato metal–biomolecule frameworks (Cu^{II}/ade–MOFs)	0.1M $NaHCO_3$		73% (Total)	[9]
		−1.4 V_{RHE}	45% (C_2H_4)	
		−1.6 V_{RHE}	50% (CH_4)	
Defective polymeric Co phthalocyanine	0.5M $KHCO_3$	−0.61 V_{RHE}	97 % (CO)	[10]
ZIF-8 (= Zeolitic imidazolate framework)	0.5M NaCl	−1.8 V_{SCE}	69.8% (CO)	[11]
ZIF-8	0.25M K_2SO_4	−1.1 V_{RHE}	81.0% (CO)	[12]
Zn–BTC MOFs	$BmimPF_6$	$-2.2\ V_{Ag/Ag+}$	92.8% (CH_4)	[13]
Fe_MOF-525 (= Fe–porphyrin–based MOF–525 Films) $[Zr_6O_4(OH)_4(TCPP)_3]$ (MOF-525, H_4TCPP = meso-tetrakis(4-carboxyphenyl)porphyrin)	1M $TBAPF_6$/acetonitrile	−1.3 V_{NHE}	54±2 % (CO)	[14]
Re-SURMOF (= $ReL(CO)_3Cl$ into highly oriented surface-grafted MOF thin films L = 2,2'-bipyridine-5,5'-dicarboxylic acid	0.1M TBAH in CH_3CN with 5% trifluoroethanol (by volume)	−1.6 V_{NHE}	93±5% (CO)	[15]
PCN-222(Fe)	0.5M $KHCO_3$	−0.60 V_{RHE}	91% (CO)	[16]
Bi-BTC-D $C_{12}H_{10}BiNO_7$	0.5M $KHCO_3$	−0.86 V_{RHE}	95.5% (HCOOH)	This work

Table S2. Crystal data and structure refinement for 20190920zh_znz4046_2_0m_a_sq.

Identification code	20190920zh_znz4046_2_0m_a_sq	
Empirical formula	C12 H10 Bi N O7	
Formula weight	489.19	
Temperature	173(2) K	
Wavelength	1.34139 Å	
Crystal system	Monoclinic	
Space group	$P2_1/n$	
Unit cell dimensions	a = 10.1416(3) Å	α= 90°.
	b = 14.7630(4) Å	β= 100.1670(10)°.
	c = 11.3618(3) Å	γ = 90°.
Volume	1674.38(8) $Å^3$	
Z	4	
Density (calculated)	1.941 Mg/m^3	
Absorption coefficient	13.954 mm^{-1}	
F(000)	912	
Crystal size	0.130 x 0.110 x 0.080 mm^3	
Theta range for data collection	4.691 to 52.994°.	
Index ranges	-12<=h<=12, -17<=k<=16, -13<=l<=13	
Reflections collected	13110	
Independent reflections	2943 [R(int) = 0.0470]	
Completeness to theta = 52.994°	99.3 %	
Absorption correction	Semi-empirical from equivalents	
Max. and min. transmission	0.3667 and 0.1821	
Refinement method	Full-matrix least-squares on F^2	
Data / restraints / parameters	2943 / 24 / 192	
Goodness-of-fit on F^2	1.065	
Final R indices [I>2sigma(I)]	R1 = 0.0283, wR2 = 0.0732	
R indices (all data)	R1 = 0.0300, wR2 = 0.0747	
Extinction coefficient	n/a	
Largest diff. peak and hole	1.805 and -1.166 $e.Å^{-3}$	

Table S3. Atomic coordinates ($\times 10^4$) and equivalent isotropic displacement parameters ($Å^2 \times 10^3$) for 20190920zh_znz4046_2_0m_a_sq. U(eq) is defined as one third of the trace of the orthogonalized U^{ij} tensor.

	x	y	z	U(eq)
Bi(1)	3928(1)	5486(1)	6041(1)	20(1)
C(1)	6724(5)	5824(4)	6858(5)	23(1)
C(2)	8045(5)	6262(4)	7262(5)	23(1)
C(3)	9151(5)	5963(4)	6797(5)	26(1)
C(4)	10397(5)	6383(4)	7163(5)	23(1)
C(5)	10516(5)	7087(4)	7980(5)	25(1)
C(6)	9415(5)	7382(4)	8441(5)	23(1)
C(7)	8187(5)	6967(4)	8075(5)	26(1)
C(8)	11581(6)	6045(4)	6678(5)	28(1)
C(9)	9532(5)	8144(4)	9332(5)	23(1)
C(10)	6405(18)	3335(13)	9837(16)	161(6)
C(11)	3990(20)	3466(15)	9803(18)	186(8)
C(12)	5022(14)	4328(8)	8411(11)	89(3)
N(1)	5120(11)	3722(7)	9337(9)	96(3)
O(1)	6636(4)	5080(3)	6330(4)	26(1)
O(2)	5684(3)	6254(3)	7090(4)	28(1)
O(3)	8570(4)	8225(3)	9918(4)	28(1)
O(4)	10522(4)	8652(2)	9456(4)	27(1)
O(5)	12739(3)	6342(3)	7127(3)	26(1)
O(6)	11453(5)	5447(3)	5886(5)	51(2)
O(7)	4147(8)	4713(4)	7944(5)	68(2)

Table S4. Bond lengths [Å] and angles [°] for 20190920zh_znz4046_2_0m_a_sq.

Bi(1)-O(5)#1	2.257(4)
Bi(1)-O(2)	2.264(4)
Bi(1)-O(3)#2	2.284(4)
Bi(1)-O(7)	2.421(5)
Bi(1)-O(6)#1	2.485(5)
Bi(1)-C(8)#1	2.734(6)
Bi(1)-C(1)	2.868(5)
C(1)-O(1)	1.247(7)
C(1)-O(2)	1.297(7)
C(1)-C(2)	1.485(7)
C(2)-C(7)	1.382(8)
C(2)-C(3)	1.393(8)
C(3)-C(4)	1.402(8)
C(3)-H(3)	0.9500
C(4)-C(5)	1.385(8)
C(4)-C(8)	1.493(7)
C(5)-C(6)	1.385(8)
C(5)-H(5)	0.9500
C(6)-C(7)	1.385(8)
C(6)-C(9)	1.503(8)
C(7)-H(7)	0.9500
C(8)-O(6)	1.251(7)
C(8)-O(5)	1.273(7)
C(9)-O(4)	1.241(6)
C(9)-O(3)	1.281(7)
C(10)-N(1)	1.444(17)
C(10)-H(10A)	0.9800
C(10)-H(10B)	0.9800
C(10)-H(10C)	0.9800
C(11)-N(1)	1.397(19)
C(11)-H(11A)	0.9800
C(11)-H(11B)	0.9800
C(11)-H(11C)	0.9800
C(12)-O(7)	1.107(13)
C(12)-N(1)	1.371(14)
C(12)-H(12)	0.9500

O(5)#1-Bi(1)-O(2)	83.02(13)
O(5)#1-Bi(1)-O(3)#2	77.98(14)
O(2)-Bi(1)-O(3)#2	84.83(15)
O(5)#1-Bi(1)-O(7)	75.48(17)
O(2)-Bi(1)-O(7)	80.0(2)
O(3)#2-Bi(1)-O(7)	150.75(18)
O(5)#1-Bi(1)-O(6)#1	54.69(14)
O(2)-Bi(1)-O(6)#1	137.70(14)
O(3)#2-Bi(1)-O(6)#1	85.47(17)
O(7)-Bi(1)-O(6)#1	89.1(2)
O(5)#1-Bi(1)-C(8)#1	27.49(15)
O(2)-Bi(1)-C(8)#1	110.51(15)
O(3)#2-Bi(1)-C(8)#1	80.60(16)
O(7)-Bi(1)-C(8)#1	81.5(2)
O(6)#1-Bi(1)-C(8)#1	27.20(16)
O(5)#1-Bi(1)-C(1)	108.57(14)
O(2)-Bi(1)-C(1)	26.04(15)
O(3)#2-Bi(1)-C(1)	94.96(15)
O(7)-Bi(1)-C(1)	82.1(2)
O(6)#1-Bi(1)-C(1)	162.85(16)
C(8)#1-Bi(1)-C(1)	135.98(16)
O(1)-C(1)-O(2)	122.4(5)
O(1)-C(1)-C(2)	121.0(5)
O(2)-C(1)-C(2)	116.5(5)
O(1)-C(1)-Bi(1)	73.0(3)
O(2)-C(1)-Bi(1)	50.0(3)
C(2)-C(1)-Bi(1)	164.2(4)
C(7)-C(2)-C(3)	119.8(5)
C(7)-C(2)-C(1)	121.0(5)
C(3)-C(2)-C(1)	119.2(5)
C(2)-C(3)-C(4)	119.4(5)
C(2)-C(3)-H(3)	120.3
C(4)-C(3)-H(3)	120.3
C(5)-C(4)-C(3)	119.9(5)
C(5)-C(4)-C(8)	121.1(5)
C(3)-C(4)-C(8)	119.0(5)
C(4)-C(5)-C(6)	120.6(5)

C(4)-C(5)-H(5)	119.7
C(6)-C(5)-H(5)	119.7
C(5)-C(6)-C(7)	119.3(5)
C(5)-C(6)-C(9)	121.1(5)
C(7)-C(6)-C(9)	119.5(5)
C(2)-C(7)-C(6)	121.1(5)
C(2)-C(7)-H(7)	119.5
C(6)-C(7)-H(7)	119.5
O(6)-C(8)-O(5)	120.2(5)
O(6)-C(8)-C(4)	120.9(5)
O(5)-C(8)-C(4)	118.9(5)
O(6)-C(8)-Bi(1)#3	65.2(3)
O(5)-C(8)-Bi(1)#3	54.9(3)
C(4)-C(8)-Bi(1)#3	173.3(4)
O(4)-C(9)-O(3)	124.0(5)
O(4)-C(9)-C(6)	119.7(5)
O(3)-C(9)-C(6)	116.3(5)
N(1)-C(10)-H(10A)	109.5
N(1)-C(10)-H(10B)	109.5
H(10A)-C(10)-H(10B)	109.5
N(1)-C(10)-H(10C)	109.5
H(10A)-C(10)-H(10C)	109.5
H(10B)-C(10)-H(10C)	109.5
N(1)-C(11)-H(11A)	109.5
N(1)-C(11)-H(11B)	109.5
H(11A)-C(11)-H(11B)	109.5
N(1)-C(11)-H(11C)	109.5
H(11A)-C(11)-H(11C)	109.5
H(11B)-C(11)-H(11C)	109.5
O(7)-C(12)-N(1)	130.3(13)
O(7)-C(12)-H(12)	114.8
N(1)-C(12)-H(12)	114.8
C(12)-N(1)-C(11)	120.9(14)
C(12)-N(1)-C(10)	119.9(13)
C(11)-N(1)-C(10)	119.2(14)
C(1)-O(2)-Bi(1)	104.0(3)
C(9)-O(3)-Bi(1)#4	107.9(3)
C(8)-O(5)-Bi(1)#3	97.6(3)

C(8)-O(6)-Bi(1)#3	87.6(3)
C(12)-O(7)-Bi(1)	127.6(8)

Symmetry transformations used to generate equivalent atoms:

#1 x-1,y,z #2 x-1/2,-y+3/2,z-1/2 #3 x+1,y,z

#4 x+1/2,-y+3/2,z+1/2

Table S5. Anisotropic displacement parameters ($Å^2 \times 10^3$) for 20190920zh_znz4046_2_0m_a_sq. The anisotropic displacement factor exponent takes the form: $-2\pi^2[h^2 a^{*2} U^{11} + ... + 2 h k a^* b^* U^{12}]$

	U^{11}	U^{22}	U^{33}	U^{23}	U^{13}	U^{12}
Bi(1)	15(1)	22(1)	24(1)	-1(1)	6(1)	1(1)
C(1)	18(3)	30(3)	23(3)	-2(2)	6(2)	-1(2)
C(2)	12(3)	27(3)	29(3)	-1(2)	5(2)	0(2)
C(3)	16(3)	28(3)	36(3)	-6(2)	9(2)	-2(2)
C(4)	12(3)	30(3)	29(3)	-4(2)	8(2)	0(2)
C(5)	18(3)	27(3)	28(3)	-4(2)	3(2)	-3(2)
C(6)	17(3)	22(3)	30(3)	-4(2)	6(2)	1(2)
C(7)	19(3)	30(3)	30(3)	-2(2)	11(2)	3(2)
C(8)	20(3)	35(3)	30(3)	-5(3)	9(2)	-1(2)
C(9)	19(3)	22(3)	27(3)	1(2)	4(2)	2(2)
C(10)	159(10)	165(10)	139(9)	5(8)	-27(8)	35(8)
C(11)	194(11)	199(12)	178(11)	5(9)	71(9)	-28(9)
C(12)	102(5)	85(5)	79(5)	1(4)	12(4)	-2(4)
N(1)	115(5)	87(4)	84(4)	6(4)	15(4)	1(4)
O(1)	19(2)	28(2)	31(2)	-4(2)	6(2)	-2(2)
O(2)	11(2)	38(2)	36(2)	-14(2)	3(2)	-2(2)
O(3)	26(2)	27(2)	34(2)	-6(2)	11(2)	-2(2)
O(4)	17(2)	22(2)	42(2)	-7(2)	6(2)	-6(2)
O(5)	12(2)	39(2)	28(2)	-8(2)	7(2)	-2(2)
O(6)	21(2)	73(4)	61(3)	-40(3)	14(2)	-7(2)
O(7)	109(5)	61(4)	40(3)	26(3)	24(3)	33(4)

Table S6. Hydrogen coordinates (x 10^4) and isotropic displacement parameters ($Å^2$x 10^3) for 20190920zh_znz4046_2_0m_a_sq.

	x	y	z	U(eq)
H(3)	9062	5480	6236	31
H(5)	11361	7370	8226	30
H(7)	7429	7171	8387	31
H(10A)	7114	3656	9521	241
H(10B)	6417	2693	9619	241
H(10C)	6558	3393	10710	241
H(11A)	3660	3986	10203	278
H(11B)	4226	2974	10380	278
H(11C)	3288	3258	9152	278
H(12)	5833	4434	8125	107

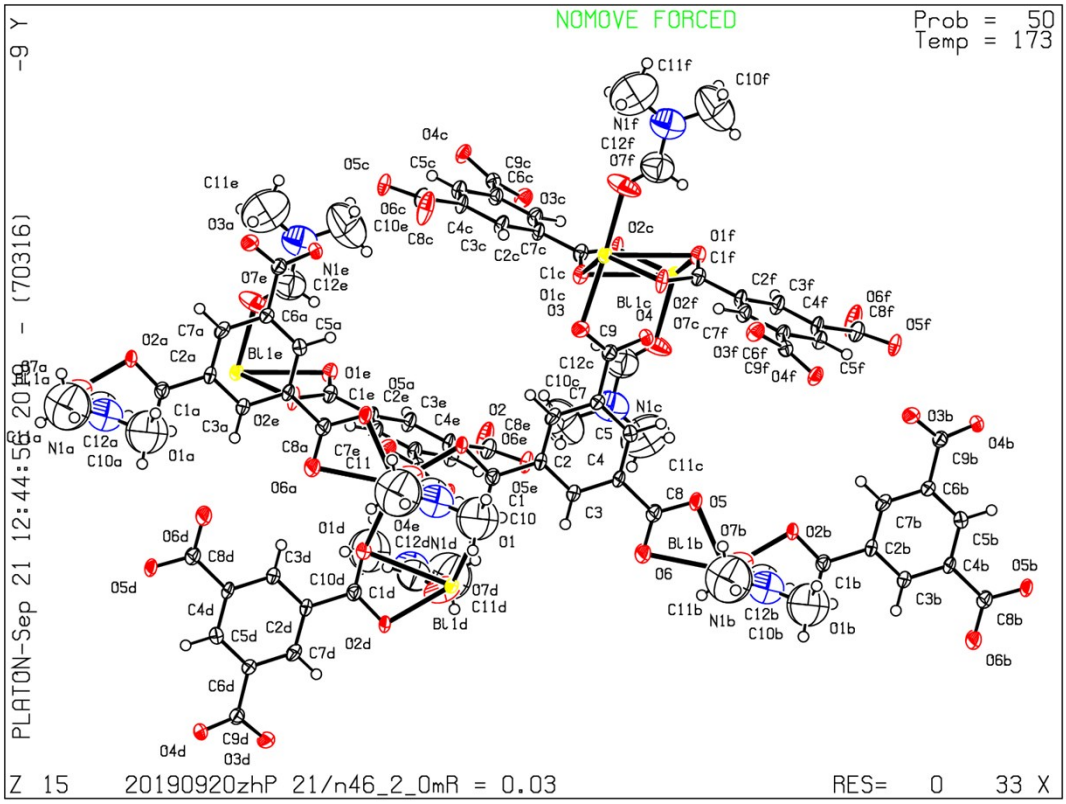

Figure S1 the Bi-BTC-D crystal structure

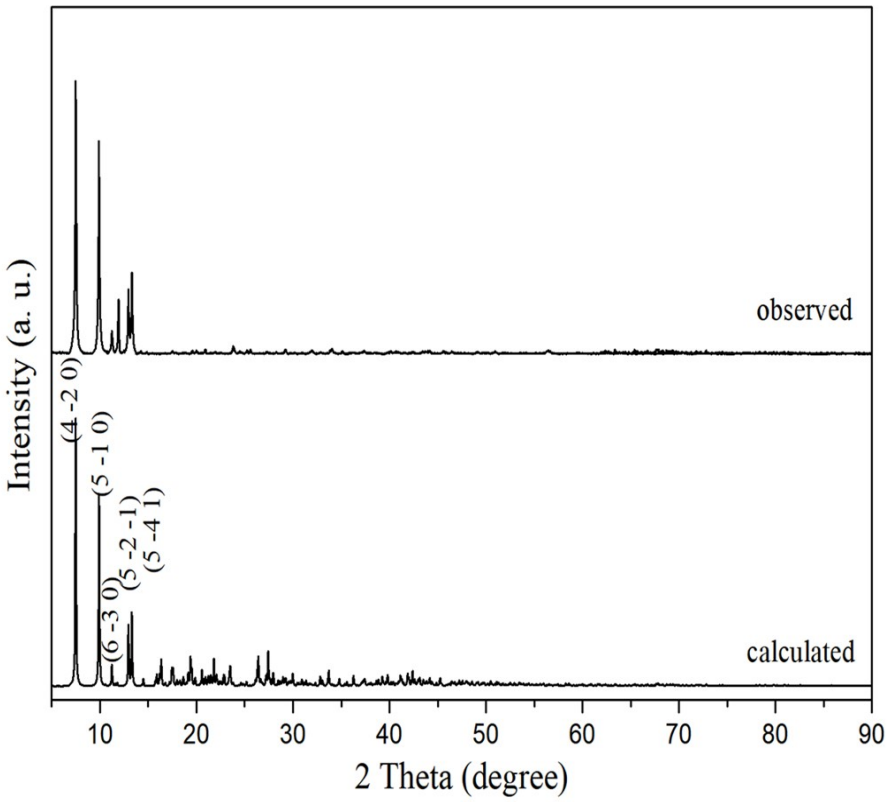

Figure S2 Observed and calculated X-ray powder diffraction of Bi-BTC.

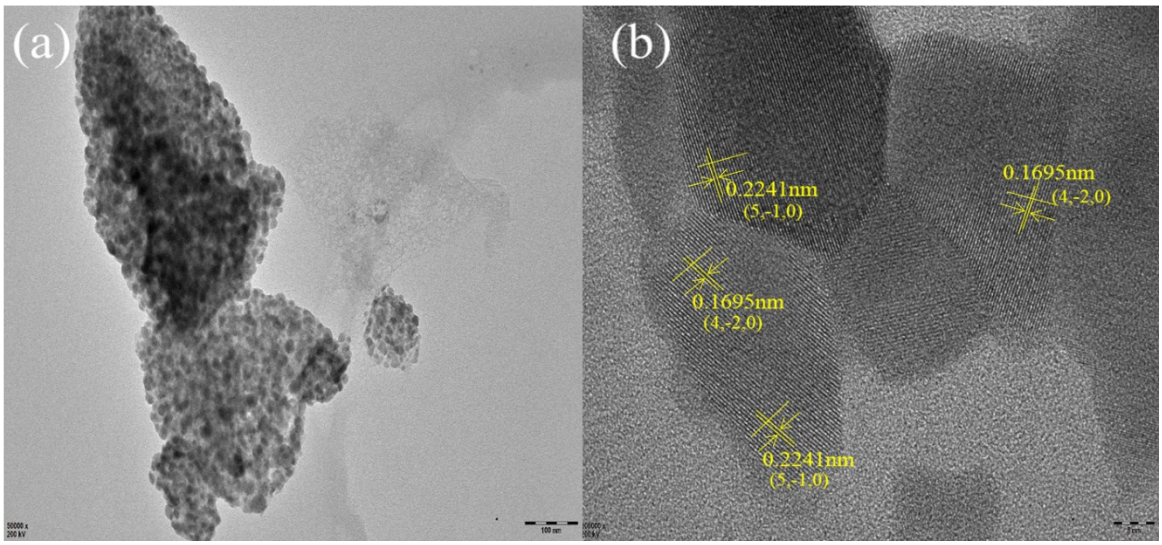

Figure S3 (a) TEM and (b) HR-TEM image of Bi-BTC composite.

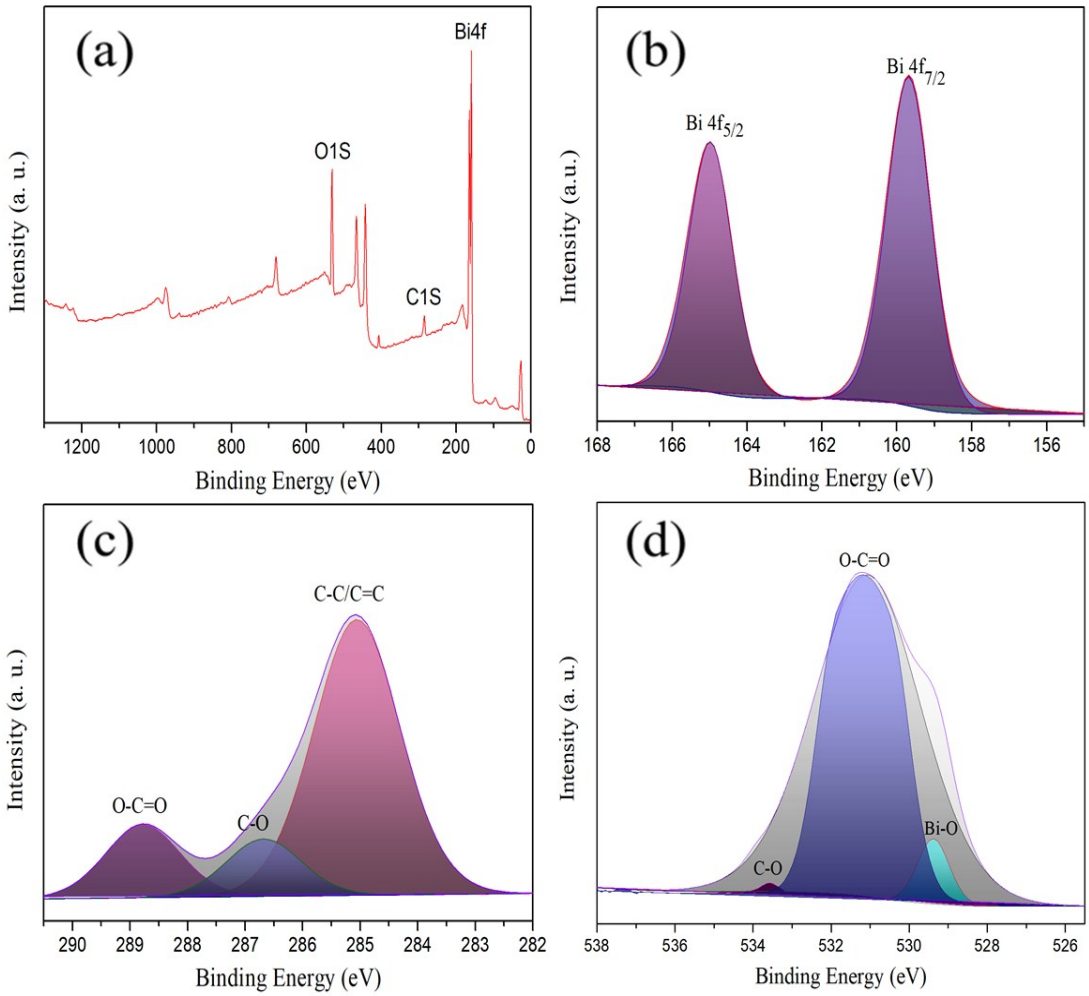

Figure S4 XPS spectra of Bi-BTC samples: (a) survey scan, (b) Bi 4f, (c) C 1s, (d) O 1s.

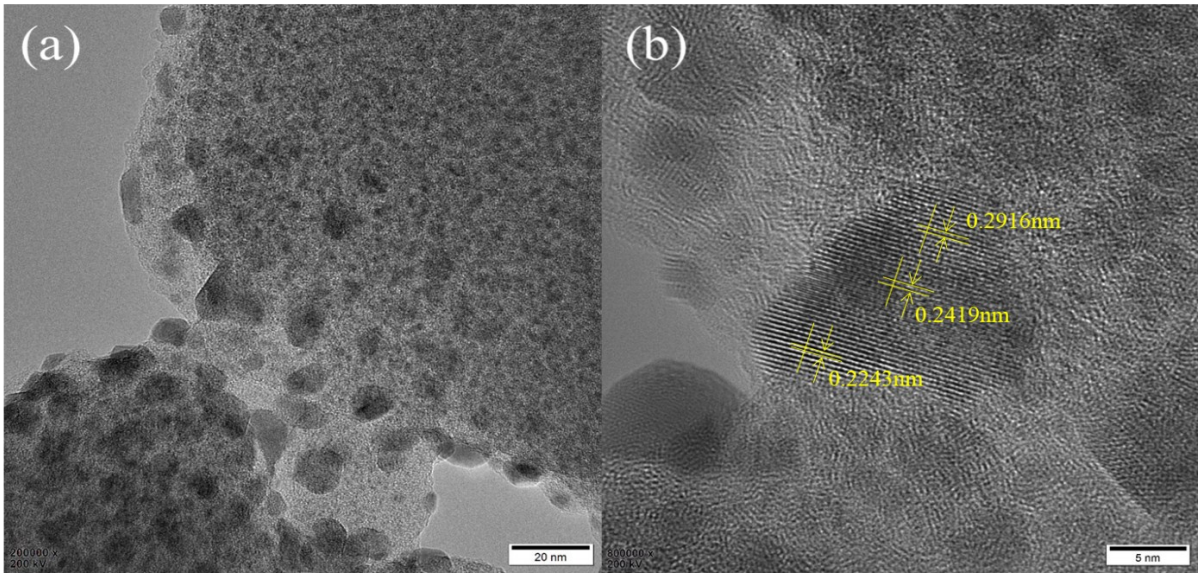

Figure S5 (a) TEM and (b) HR-TEM image of Bi-BTC composite after CO_2 reduction.

Reference

1. J. Albo, D. Vallejo, G. Beobide, O. Castillo, P. Castano and A. Irabien, *ChemSusChem*, 2017, **10**, 1100-1109.
2. D. H. Nam, O. S. Bushuyev, J. Li, P. De Luna, A. Seifitokaldani, C. T. Dinh, F. P. Garcia de Arquer, Y. Wang, Z. Liang, A. H. Proppe, C. S. Tan, P. Todorovic, O. Shekhah, C. M. Gabardo, J. W. Jo, J. Choi, M. J. Choi, S. W. Baek, J. Kim, D. Sinton, S. O. Kelley, M. Eddaoudi and E. H. Sargent, *J Am Chem Soc*, 2018, **140**, 11378-11386.
3. Y. L. Qiu, H. X. Zhong, T. T. Zhang, W. B. Xu, P. P. Su, X. F. Li and H. M. Zhang, *Acs Appl Mater Inter*, 2018, **10**, 2480-2489.
4. R. S. Kumar, S. S. Kumar and M. A. Kulandainathan, *Electrochem Commun*, 2012, **25**, 70-73.
5. J. X. Wu, S. Z. Hou, X. D. Zhang, M. Xu, H. F. Yang, P. S. Cao and Z. Y. Gu, *Chem Sci*, 2019, **10**, 2199-2205.
6. J. Albo, M. Perfecto-Irigaray, G. Beobide and A. Irabien, *Journal of Co2 Utilization*, 2019, **33**, 157-165.
7. R. Hinogami, S. Yotsuhashi, M. Deguchi, Y. Zenitani, H. Hashiba and Y. Yamada, *Ecs Electrochem Lett*, 2012, **1**, H17-H19.
8. K. Zhao, Y. Liu, X. Quan, S. Chen and H. Yu, *Acs Appl Mater Inter*, 2017, **9**, 5302-5311.
9. F. Yang, A. Chen, P. L. Deng, Y. Zhou, Z. Shahid, H. Liu and B. Y. Xia, *Chem Sci*, 2019, **10**, 7975-7981.
10. H. H. Wu, M. Zeng, X. Zhu, C. C. Tian, B. B. Mei, Y. Song, X. L. Du, Z. Jiang, L. He, C. G. Xia and S. Dai, *Chemelectrochem*, 2018, **5**, 2717-2721.
11. Y. Wang, P. Hou, Z. Wang and P. Kang, *Chemphyschem*, 2017, **18**, 3142-3147.
12. X. L. Jiang, H. B. Li, J. P. Xiao, D. F. Gao, R. Si, F. Yang, Y. S. Li, G. X. Wang and X. H. Bao, *Nano Energy*, 2018, **52**, 345-350.
13. X. Kang, Q. Zhu, X. Sun, J. Hu, J. Zhang, Z. Liu and B. Han, *Chem Sci*, 2016, **7**, 266-273.
14. I. Hod, M. D. Sampson, P. Deria, C. P. Kubiak, O. K. Farha and J. T. Hupp, *Acs Catalysis*, 2015, **5**, 6302-6309.
15. L. Ye, J. X. Liu, Y. Gao, C. H. Gong, M. Addicoat, T. Heine, C. Woll and L. C. Sun, *Journal of Materials Chemistry A*, 2016, **4**, 15320-15326.
16. B. X. Dong, S. L. Qian, F. Y. Bu, Y. C. Wu, L. G. Feng, Y. L. Teng, W. L. Liu and Z. W. Li, *Acs Applied Energy Materials*, 2018, **1**, 4662-4669.